Provenance of the Late Paleocene Matanomadh Sandstones, Kachchh, Western India

V. K. Srivastava, B. P. Singh and A. Patra

Abstract The late Paleocene clastic member of the Matanomadh Formation (MF) is an overall sandstone dominated succession wherein sub-ordinate proportion of thinly-laminated silty-mudstones is found lying between the sandstone beds. Provenance of these late Paleocene Matanomadh Sandstones (MS), Kachchh is not known till date and the same has been determined based on petrography and heavy mineral analysis supported by paleocurrent studies. These sandstones reveal an abundance of sub-angular to rounded monocrystalline non-undulatory quartz; and polycrystalline quartz, feldspar and rock fragments occur as minor constituents. These sandstones are classified as quartzose arenite. The rock fragments in these sandstones are dominated by mica-schist, slate, chert and limestones. Q-F-L and Qm-F-Lt diagrams suggest margin of the craton interior to transitional continental stable craton provenance for these sandstones. The paleocurrent measurements of the cross-bedded sandstones suggest NW-SE-directed bipolar and WNW-directed unimodal paleocurrent patterns and suggest a marine-continental transition zone as depositional site for these sandstones where sediments were contributed from both the shallow-marine and continental sources. The heavy mineral assemblages of these sandstones show sub-angular to rounded grains of magnetite, tourmaline, monazite, rutile, kyanite, staurolite and hematite where magnetite is the dominant component; and hence suggest that the heavy minerals might have been supplied from a basic igneous source, low- to medium-grade metamorphic rocks and reworked sedimentary rocks.

Keywords Matanomadh sandstones · Late Paleocene
Kachchh basin · Western India · Heavy minerals · Paleocurrent

V. K. Srivastava · B. P. Singh (✉) · A. Patra
Centre of Advanced Study in Geology, Banaras Hindu University, Varanasi 221005, India
e-mail: drbpsingh1960@gmail.com

S. Bajpai et al. (eds.), *The Indian Paleogene*, Society of Earth Scientists Series,
https://doi.org/10.1007/978-3-319-77443-5_6

Introduction

Matanomadh Formation represents the lowermost lithostratigraphic unit of the Tertiary succession of Kachchh and is assigned Paleocene age (Fig. 1). It has been subdivided into a basal lateritic member and an upper clastic member by Saxena (1975). Matanomadh sandstones (MS) whose provenance determination has been attempted in the present study, are exposed along Nakhatrana-Lakhpat road section (N 23° 32′ 43″ E 68° 57′ 04″) and also in the badlands east of the Matanomadh village (N 23° 32′ 06″ E 68° 58′ 16″) in the Kachchh district, Gujarat. Wynne (1872) was the first who studied these Paleocene rocks of Kachchh basin exposed around Matanomadh village and classified them as Sub-Nummulitic Group. Thereafter, Biswas (1965) and Biswas and Raju (1973) proposed a new Time-Stratigraphic classification for the Tertiary sequences of Kachchh and modified it as Madh Series. Recently, Biswas (1992) classified this succession as Matanomadh Formation (MF), after its type area Matanomadh village which is situated at the north-western margin of the Kachchh peninsula (Fig. 1). Lateritic member of the Matanomadh Formation is ~10 m thick and consists of variety of light coloured calcareous and ferruginous mudstones. Laterite and bauxite beds occur in between these mudstones. The clastic member is comprised of a ~17 m thick succession of horizontally-bedded and cross-bedded sandstones, including herringbone cross-bedding and silty-mudstones (Srivastava and Singh 2017) (Fig. 2).

Provenance analysis includes all enquiries that would aid in reconstructing the lithospheric history of the Earth (Basu 2003; Weltje and Eynatten 2004) and can be performed with the help of detrital minerals, including heavy minerals supported by paleocurrent analysis. Provenance studies of sedimentary rocks have chiefly taken into account the mineralogical and/or chemical composition of sandstones and shales (Basu 1976; Dickinson and Suczek 1979; Dickinson et al. 1983; Singh 1996, 2013; Singh et al. 2000; Srivastava and Pandey 2011; Jalal and Ghosh 2012). Provenance study includes the distance and direction of transport, size and setting of the source region, climate and relief in the source area and the specific types of source rocks (Pettijohn et al. 1987). Additionally, heavy minerals have been utilized in provenance studies by numerous workers (e.g. Morton 1985; Basu and Molinaroli 1989; Nechaev and Isphording 1993; Singh et al. 2004; Patra et al. 2014).

Although biostratigraphic aspects of the Paleogene succession in Kachchh are well studied; its sedimentological aspects are least focused. Since little work has been carried out on these sandstones and the determination of provenance for the Matanomadh sandstones has not been attempted until now, authors aim to provide an insight on its plausible provenance. Therefore, an attempt is being made here to illustrate the plausible provenance using light and heavy minerals analysis, rock fragments and paleocurrent analysis as the major tools.

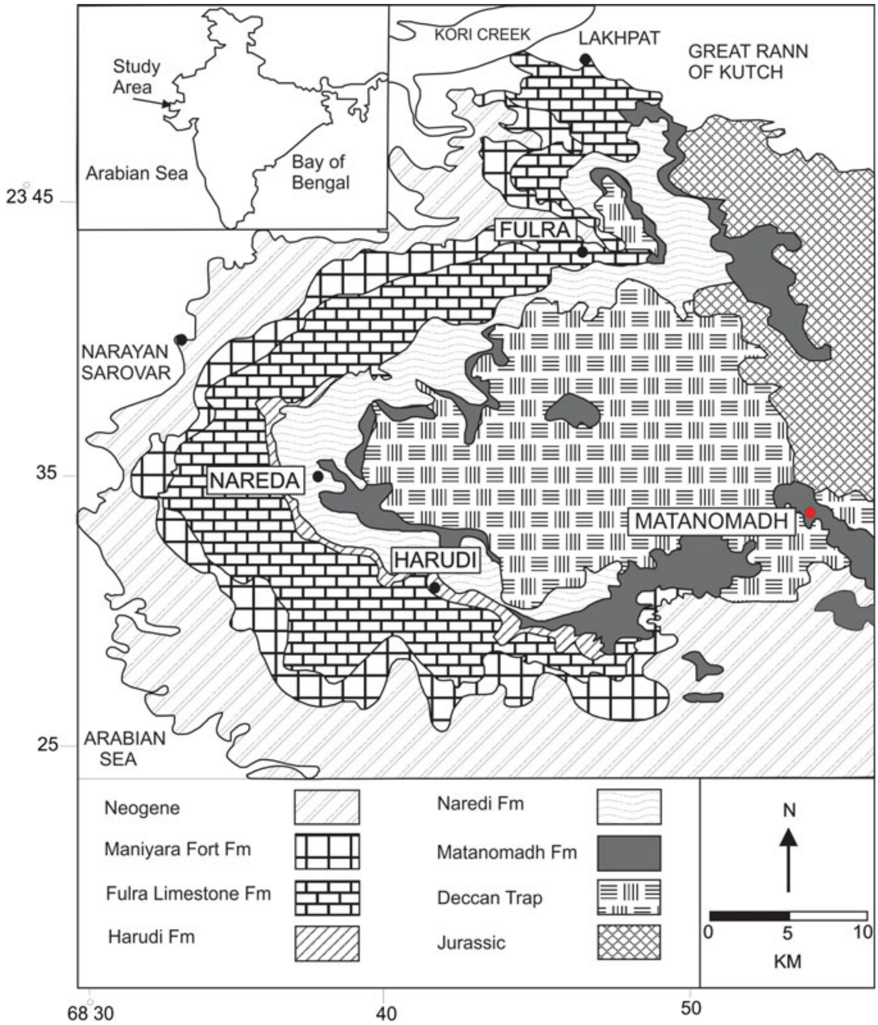

Fig. 1 Geological map showing Paleogene outcrops in the western Kachchh (after Biswas 1992). Here Matanomadh Formation is shown in grey patches. Red circle represents the investigated area. Inset: India in the outline map and arrow indicates the study area

Geological Background

Pericratonic Kachchh basin (KB), extended between latitudes 22° 30′ and 24° 30′N and longitudes 68° and 72°E, evolved due to sequential rifting and repeated movements in relation with the northward drift of Indian plate after the breakup of the Gondwanaland during Late Triassic-Early Jurassic period (~200 ma) (Norton and Sclater 1979; Biswas 1982, 1987). KB is bounded by the Nagar-Parkar fault in

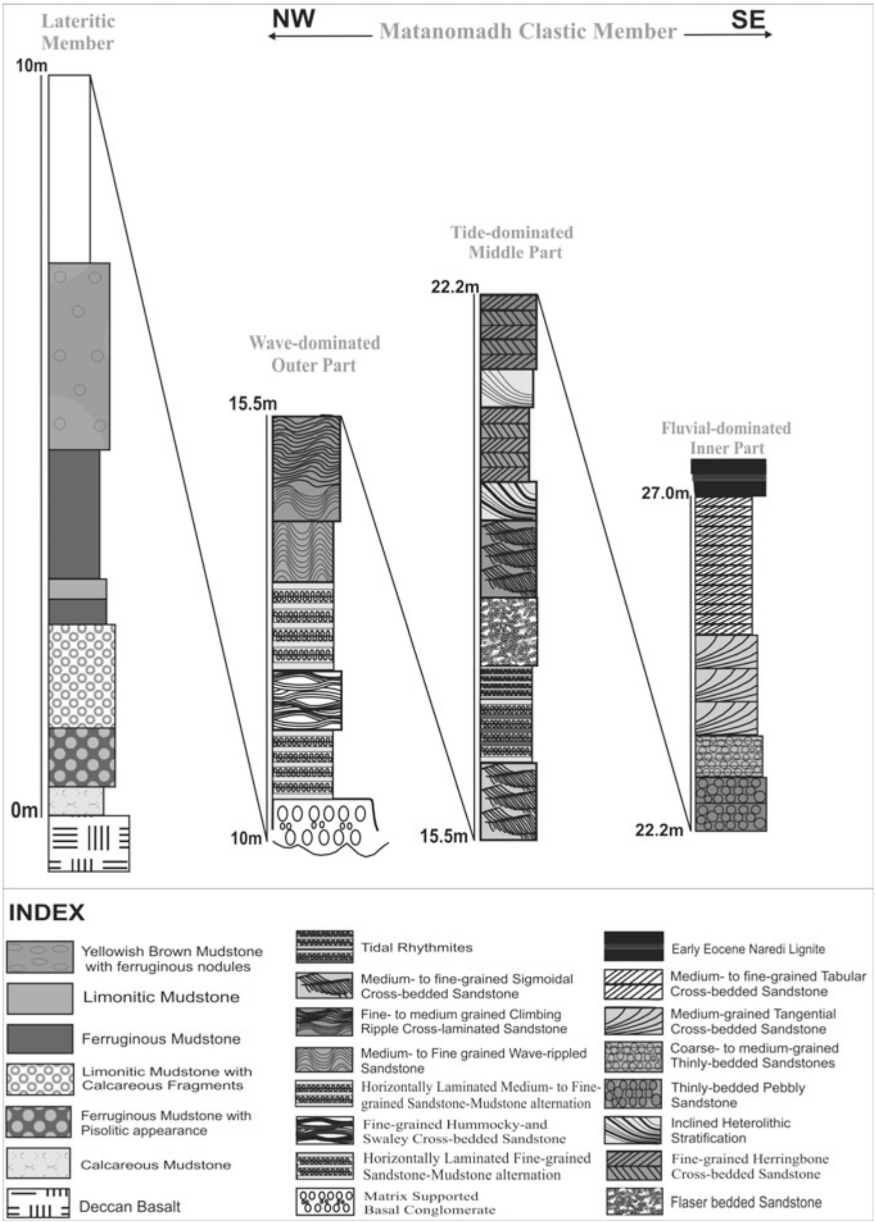

Fig. 2 Lithocolumn exhibiting vertical architecture of different lithofacies in the Paleocene succession of the Matanomadh Formation, Kachchh, including the late Paleocene sandstones of the Matanomadh Clastic Member

the North, Radhanpur-Barmer arch in the east and North Kathiawar fault towards the south (Biswas 1982). The basin has extended far offshore into the Arabian Sea in the west. It has preserved almost a complete sequence from middle-Jurassic to Recent punctuated by several stratigraphic breaks between transgressive cycles. The western marginal Kachchh basin constitutes one of the best developed, undisturbed Mesozoic-Cenozoic sequences in India and provides the repository of geological records related to the Gondwanaland fragmentation (Biswas 2005).

The Tertiary sequences are developed in the western part of this basin and exposed mainly in the narrow coastal plains of Kachchh Mainland and in the peripheral plains of other Mesozoic highlands (Biswas 1992). A complete section of the late Paleocene Matanomadh Clastic Member is outcropped in the western part of the Kachchh Mainland bordering Deccan Basalt (Fig. 1). The ~27 m thick MF represents the oldest lithostratigraphic unit of the Tertiary sequence of Kachchh (Fig. 1) and has been divided into a basal Lateritic Member and an upper Clastic Member (Saxena 1975). The basal lateritic member is about 10.0 m thick and is composed of calcareous mudstone, ferruginous mudstone, bauxite and laterite deposits. Clastic member in the upper part is comprised of ~17 m thick succession of sandstones and sandstone-mudstone alternation that are exposed in the eastern side of the Matanomadh village. The MF is overlain by Eocene lignite-containing Naredi Formation in the western part of the study area (Biswas 1992) where these lignite deposits are being mined by Gujarat Mineral and Development Corporation at Matanomadh and Panandhro localities.

Methodology

Individual facies were identified in the field and underlying and overlying facies were demarcated considering their sedimentologic attributes such as lithology, texture and sedimentary structures and based on that a detailed litholog was prepared. Fresh samples of these late Paleocene sandstones were collected from exposed sections. A total of 12 representative samples were used for thin section preparation for petrographic study out of the total 65 collected samples. Modal analysis was carried out with the help of Image Analysis Software attached with Leica Polarizing Microscope. Heavy minerals were separated from the sandstones using heavy liquid separation method. The sandstone was disaggregated by gently grinding it and the disaggregated fraction was sieved to obtain a size range of 0.0125–0.088 mm. The sieved fraction was then poured in the heavy liquid (Bromoform in the present study having Sp. Gr. 2.89) containing separating funnel. The liquid was stirred with a glass rod for proper mixing and heavy minerals were allowed to settle at the bottom of the funnel for nearly 20 min. This process was repeated three-times and subsequently, the settled heavy minerals were collected on a filter paper and dried at room temperature. Later on, they were washed with acetone to remove coatings. The heavy minerals were then mounted on glass slides with canada balsam. For paleocurrent measurements, the azimuthal data and angle of inclination were recorded for each cross-bed at different locations along and across facies boundaries.

Results

Matanomadh sandstone occurs as planar-bedded, cross-bedded, and ripple cross-laminated and laminated sandstones. Petrography, heavy mineral and paleocurrent analysis of these sandstones was performed and the results are described as under.

Petrography

Matanomadh sandstones are hard and compact and show unimodal to bimodal distribution of the particles (Figs. 3 and 4). Two varieties of the sandstones can be identified as coarse- to medium-grained sandstone and medium- to fine-grained sandstone on the basis of the particle size variation. Coarse to medium framework grains form the thickly- and thinly-bedded sandstones, and cross-bedded sandstones, while medium to fine framework grains form the ripple cross-laminated and laminated sandstones. The coarse- to medium-grained sandstone is moderately sorted and the grains are sub-rounded to rounded, show bimodal distribution (Fig. 3a). A few well rounded grains are also found. In them, quartz forms 74–75% where monocrystalline quartz (~67%) dominates over polycrystalline (8%) and non-undulatory quartz grains dominate over undulatory quartz. Polycrystalline quartz show interlocking texture. Low amount of feldspar (11–12%) is present in these sandstones (Table 1), which are mainly microcline and plagioclase (Fig. 3b, c), including the weathered varieties (Fig. 3d). Rock fragments form a little proportion (2–3%) in the coarse- to medium-grained sandstone. Cement (12–13%), is mainly calcareous and ferruginous in this variety of sandstones. These can be classified as quartzose arenites (following Okada 1971).

In the medium- to fine-grained sandstone, framework grains are mainly sub-angular to sub-rounded (Fig. 4). Quartz forms 76–78% where monocrystalline variety (~74%) dominates over the polycrystalline (~4%) in them (Table 1) (Fig. 4a). Mica is mainly muscovite in these sandstones (Fig. 4b–d). The rock-fragments of mica-schist and chert are observed in addition to few limestone fragments (Fig. 4c, d). Feldspar forms about 5% and rock fragments form 6–8% in this type of sandstone. Cementing material (11–12%) is mainly carbonate and iron-oxide. In some samples only carbonate cement is present, while in others, iron oxide coatings are present over the particles and cement is mainly carbonate. In those sandstones, which contain both the types of cement the carbonate cement looks earlier precipitated than ferruginous cement. The sandstones composition suggests that they belong to quartzose arenite types (after Okada 1971).

Table 1 Modal composition of the Matanomadh sandstones

Constituents (in %)	Coarse- to medium-grained sandstones						Medium- to fine-grained sandstones					
Quartz (Qtz)	73.91	74.55	74.32	74.36	74.13	74.56	78.03	76.82	77.45	75.84	75.79	75.55
Poly. Qtz	8.09	8.22	8.16	7.94	7.78	8.00	3.54	3.31	3.07	3.02	3.08	2.43
Mono. Qtz	65.82	66.33	66.16	66.42	66.40	66.56	74.49	73.51	74.38	72.82	72.71	73.12
Und. Qtz	8.62	7.83	8.22	7.80	8.08	8.16	5.21	5.91	5.46	5.20	5.42	5.32
Non-Und. Qtz	65.29	66.72	66.10	66.56	66.05	66.40	72.82	70.92	71.99	70.64	70.37	70.23
Feldspar	12.01	11.92	12.05	11.47	10.63	10.32	4.43	4.93	4.78	4.02	4.54	4.85
Rock Frag. (m)	–	0.40	0.51	0.53	1.02	0.84	4.26	4.57	4.21	5.94	5.48	6.03
Rock Frag. (s)	1.05	1.02	0.94	0.80	1.24	1.34	2.08	2.29	2.06	2.19	2.45	2.18
Rock Frag. (i)	–	–	–	–	–	–	–	–	–	–	–	–
Carbn. Cement	7.00	6.63	6.76	9.49	9.48	9.32	9.06	9.12	9.27	8.50	8.28	8.36
Ferrug. Cement	6.03	5.48	5.42	3.35	3.50	3.62	2.14	2.27	2.23	3.51	3.46	3.03
Total	100	100	100	100	100	100	100	100	100	100	100	100

Qtz = Quartz; Poly. Qtz = Polycrystalline Quartz; Mono. Qtz = Monocrystalline Quartz; Und. Qtz = Undulatory Quartz; Non-Und. Qtz = Non-undulatory Quartz; Frag. = Fragments; m = metamorphic; s = sedimentary; i = igneous; Carbn. = Carbonate; Ferrug. = Ferruginous

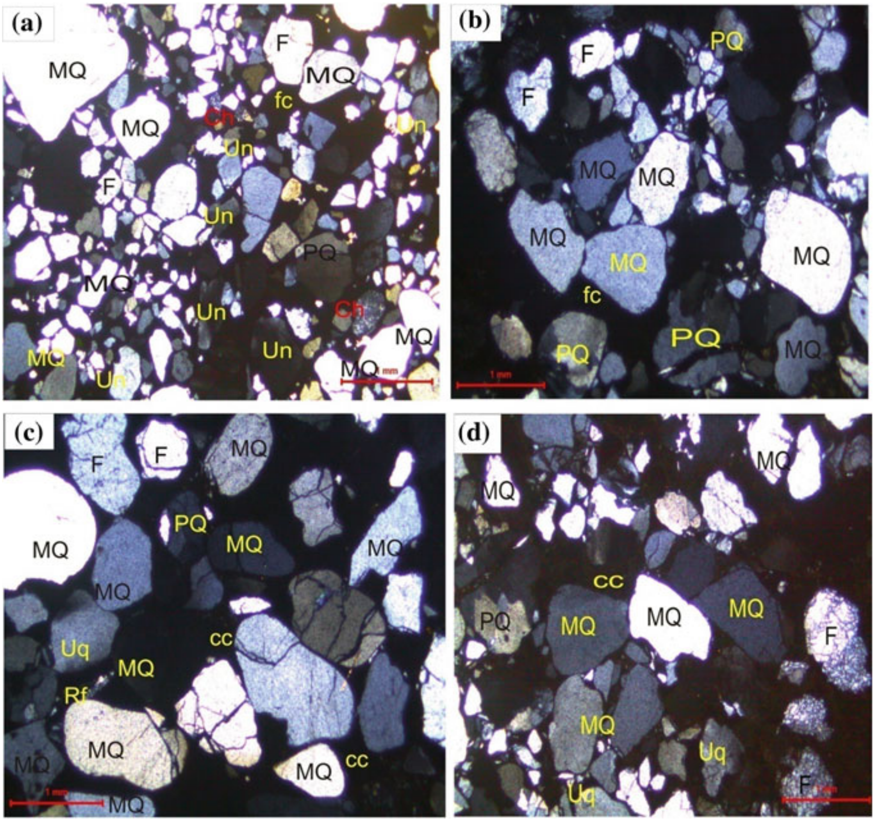

Fig. 3 Photomicrographs of coarse- to medium-grained sandstones. **a** Photomicrograph showing bimodal nature of grain size distribution and dominantly possessing monocrystalline quartz (MQ), polycrystalline quartz (PQ), undulatory quartz (Un), feldspar (F) and chert (Ch) cemented by ferruginous cement (fc). **b** Photomicrograph dominantly possessing sub-angular to sub-rounded monocrystalline quartz (MQ), polycrystalline quartz (PQ), undulatory quartz (Un), feldspar (F) cemented by ferruginous cement (fc). **c** Photomicrograph possessing sub-rounded monocrystalline quartz (MQ), polycrystalline quartz (PQ), undulatory quartz (Un) and feldspar (F) cemented by calcareous cement (cc). **d** Photomicrograph possessing sub-rounded monocrystalline quartz (MQ), polycrystalline quartz (PQ), undulatory quartz (Un) and weathered feldspar (F) cemented by calcareous cement (cc)

In Q-F-L diagram (after Dickinson et al. 1983), the composition of these sandstone units occupy the position within the craton interior (Fig. 5a) (Table 2). Further, they occupy craton interior to transitional continental field in the Qm-F-Lt diagram following Dickinson et al. (1983) (Table 3) (Fig. 5b).

Table 2 Recalculated data with respect to Q-F-L components in the Matanomadh sandstones (after excluding cement proportion)

Constituents (in %)	Coarse- to medium-grained sandstones						Medium- to fine-grained sandstones					
Q	84.98	84.82	84.63	85.31	85.19	85.64	87.87	86.69	87.51	86.19	85.87	85.26
F	13.80	13.56	13.72	13.16	12.21	10.32	4.99	5.56	5.40	4.57	5.15	5.47
L	1.22	1.62	1.65	1.53	2.60	4.04	7.14	7.75	7.09	9.24	8.98	9.27
Total	100	100	100	100	100	100	100	100	100	100	100	100

Q = Total Quartz; F = Feldspar; L = Rock fragments

Table 3 Recalculated data with respect to Qm-F-Lt components in the Matanomadh sandstones

Constituents (in %)	Coarse- to medium-grained sandstones						Medium- to fine-grained sandstones					
Qm	75.65	75.45	75.33	76.20	76.30	76.45	83.88	82.95	84.04	82.76	82.38	82.52
F	13.80	13.56	13.72	13.16	12.21	10.32	4.99	5.56	5.40	4.57	5.15	5.47
Lt	10.55	10.99	10.95	10.64	11.49	11.85	11.13	11.49	10.56	12.67	12.47	12.01
Total	100	100	100	100	100	100	100	100	100	100	100	100

Qm = Quartz monocrystalline; F = Feldspar; Lt = Rock fragments including quartzite fragments (polycrystalline quartz)

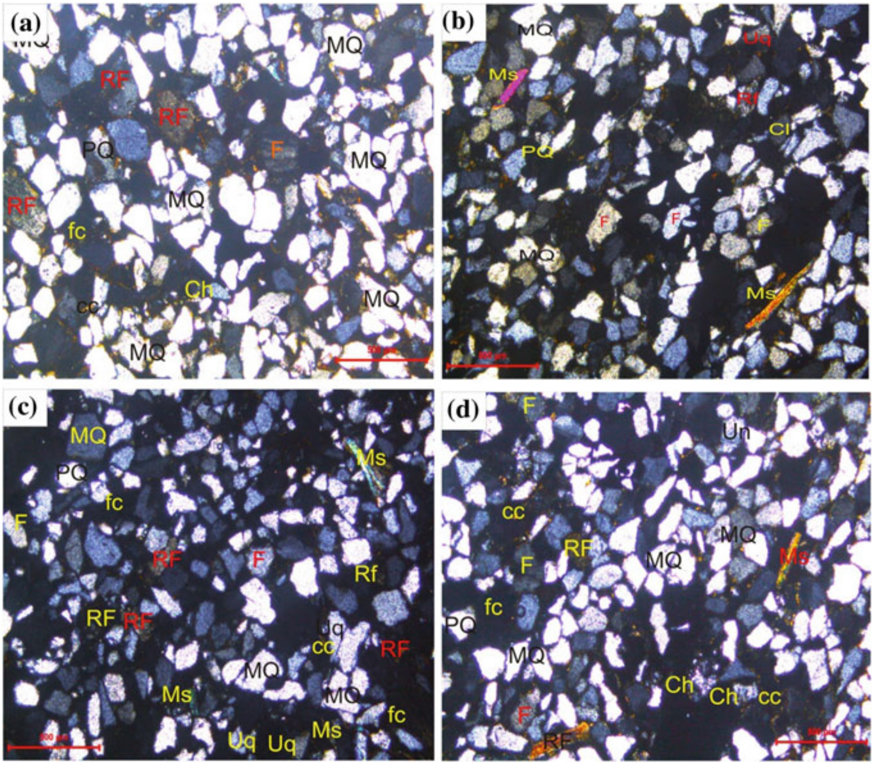

Fig. 4 Photomicrographs of medium- to fine-grained sandstones. **a** Photomicrograph shows sub-angular to sub-rounded monocrystalline quartz (MQ), polycrystalline quartz (PQ), feldspar (F) and rock fragments phyllite (RF)/chert (Ch) cemented by both calcareous and ferruginous cement. **b** Photomicrograph shows sub-angular to sub-rounded monocrystalline quartz (MQ), polycrystalline quartz (PQ), undulatory quartz (Un), feldspar (F) and rock fragments (RF)/calcite (Cl) and muscovite (Ms) cemented by both calcareous and ferruginous cement. **c** Photomicrograph shows sub-angular to sub-rounded monocrystalline quartz (MQ), polycrystalline quartz (PQ), undulatory quartz (Un), feldspar (F) and rock fragments (RF) and muscovite (Ms) cemented by both calcareous and ferruginous cement. **d** Photomicrograph shows sub-angular to sub-rounded monocrystalline quartz (MQ), polycrystalline quartz (PQ), undulatory quartz (Un), feldspar (F) and rock fragments (RF)/chert (Ch) and muscovite (Ms) cemented by both calcareous and ferruginous cement

Heavy Minerals

In these sandstones, both opaque and non-opaque heavy mineral varieties occur where opaque variety dominates over non-opaque. In particular, the proportion of opaque heavy minerals (magnetite) increases up-section and the proportions of non-opaque heavy minerals decrease up-section. Most of the studied heavy minerals are sub-rounded in outline but some of them show sub-angular and rounded forms also.

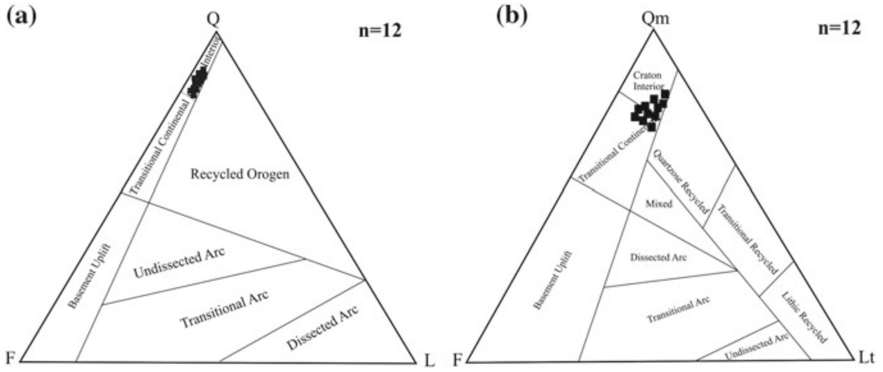

Fig. 5 **a** Q-F-L diagram for the late Paleocene Matanomadh Sandstones, Kachchh basin (after Dickinson et al. 1983). Here n represents the number of samples. **b** Qm-F-Lt diagram for the late Paleocene Matanomadh Sandstones, Kachchh basin (after Dickinson et al. 1983). Here n represents the number of samples

In order of abundance, the heavy minerals suite is comprised of magnetite > tourmaline > kyanite > rutile > monazite > staurolite > hematite (Table 4).

Magnetite ranges from 55 to 66% with sub-angular to sub-rounded nature of the grain corners. It is identified by its black colour and high relief (Fig. 6). Tourmaline occurs in a range of 9–15% and shows sub-rounded to rounded grain boundaries. Two varieties of tourmaline are identified; they are yellow to brown and blue tourmaline. It is identified by its pleochroism, high refractive index, imperfect cleavage and parallel extinction (Fig. 6). Kyanite forms 6–11% of the heavy minerals with sub-rounded shape. It is recognized by its bladed form, colour, oblique extinction and two-sets of mutually perpendicular cleavage pattern (Fig. 6). Rutile occurs in a range of 6–12% with sub-rounded to rounded grain boundaries. It is identified by its characteristic deep red interference colour and pleochroism (Fig. 6). Monazite forming 6–10% of the heavy minerals shows prismatic crystal outline with sub-rounded to rounded grain shape and recognized by its greenish black colour and shining surface (Fig. 6). Staurolite forms 2–4% of the bulk heavy minerals. It shows yellowish colour, angular shape, pleochroism, high refractive index, imperfect cleavage, low birefringence and parallel extinction. It contains numerous inclusions of quartz (Fig. 6). Hematite ranges from 1 to 3% and it shows angular to sub-angular nature of corners. It is identified by its light reddish grain boundaries (Fig. 6).

Dispersal Pattern

Sediments dispersal pattern is mainly controlled by flow directions and hydrodynamic conditions of the depositional processes and depositional milieu. Flow directions in sedimentary successions are commonly associated with primary sedimentary

Table 4 Heavy minerals percentage in the Matanomadh sandstones

Constituents (in %)	Coarse- to medium-grained sandstones						Medium- to fine-grained sandstones					
Magnetite	66	66	65	56	57	57	56	55	55	56	57	56
Tourmaline	10	9	9	13	13	12	11	12	12	14	14	15
Kyanite	7	7	6	11	10	10	9	9	9	8	8	8
Rutile	6	7	7	8	9	10	12	11	12	12	11	11
Monazite	9	9	10	7	6	6	7	7	7	6	7	6
Staurolite	–	–	–	2	3	3	2	3	3	3	3	4
Hematite	2	2	3	3	2	2	3	3	2	1	–	–
Total	100	100	100	100	100	100	100	100	100	100	100	100

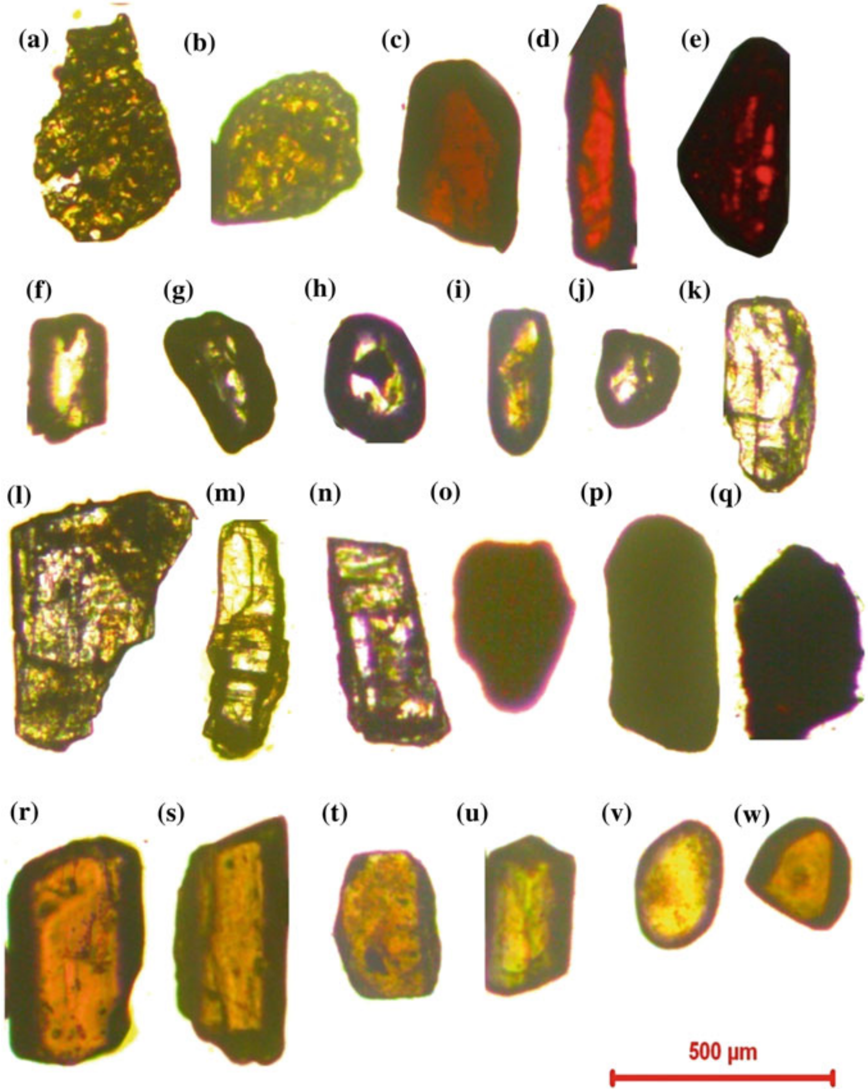

Fig. 6 Heavy minerals. **a**, **b** Staurolite; **c**–**e** Rutile; **f**–**j** Monazite; **k**–**n** Kyanite; **o** Hematite; **p**, **q** Magnetite; **r**–**w** Tourmaline

structures (Selley 1980; Pettijohn 1984) and these structures are the only direct source for paleocurrent measurements. The dispersal/paleocurrent pattern measured from the foresets of the Matanomadh cross-bedded sandstones decipher NW-SE, NW and WNW-ESE directed bipolar and unidirectional paleocurrent patterns. The paleocurrent reversal is the characteristic feature of the lower part of the succession which is dominated by sigmoidal- and herringbone cross-beds (Fig. 7a). The NW-directed

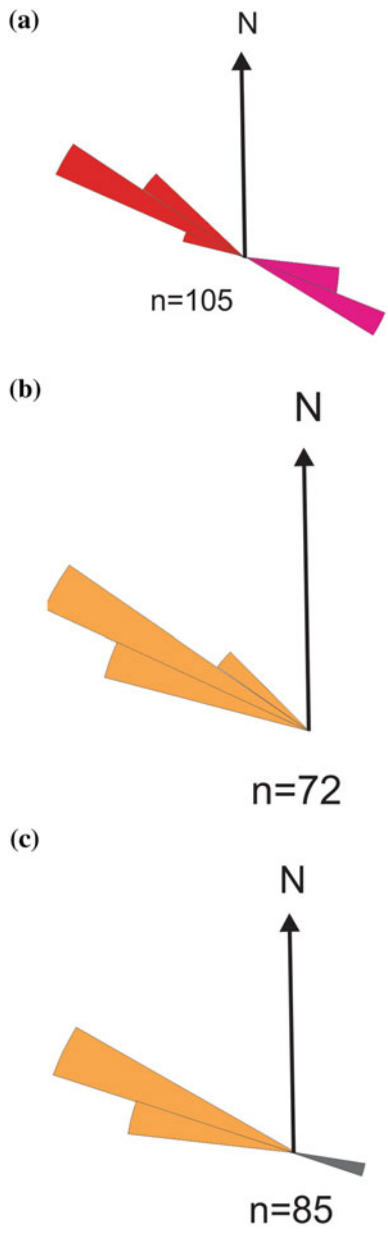

Fig. 7 Paleocurrent diagrams. **a** Paleocurrent diagram for the herringbone- and sigmoidal cross-bedded sandstones. Note here the bipolar dispersal pattern from the tide-dominated lower part of the succession. **b** Paleocurrent diagram for the tangential cross-bedded sandstones. **c** Paleocurrent diagram for the tabular cross-bedded sandstones. Note here the unidirectional dispersal pattern from the fluvial-dominated upper part of the Matanomadh sandstone succession

unidirectional paleocurrent (Fig. 7b) and the WNW-dominated bipolar paleocurrent pattern are observed in the upper part of the succession containing tangential and tabular cross-beds (Fig. 7c).

Discussion

Provenance for the MS is discussed based on the light minerals, rock fragments and heavy minerals analysis. The occurrence of quartz having monocrystalline non-undulatory nature generally points towards sources such as volcanic and hypabasal igneous rocks, fine-grained schists, phyllite and slates, and pre-existing sedimentary rocks (e.g. Blatt et al. 1980). The polycrystalline quartz with interlocking texture is derived from a metamorphic rock, most likely quartzite (e.g. Blatt et al. 1980). Chert in these rocks would have been derived from sedimentary rocks. Plagioclase variety of feldspar might have derived from a basaltic source. The limestone fragments suggest their derivation from a sedimentary source. The metamorphic rocks of the Aravalli hills exposed in the NE must have acted as the chief sources for the MS. Deccan Trap forms the basement of the MF in the Kachchh region. In the Kachchh region, Deccan trap is defined as the outpouring of tholeiitic basaltic lava that overlies the Mesozoic sedimentary rocks of marine and fluvio-deltaic origin (Merh 1995). This must have contributed part of the sediments to the MS.

Kachchh Basin is an east-west oriented pericratonic rift basin at the western-most periphery of the Indian subcontinent. The Kachchh Rift evolved within the Mid-Proterozoic Aravalli-Delhi fold belt by reactivation of pre-existing faults along NE-SW trend of Delhi fold belt that swings to E-W in Kachchh region (Biswas 2005).Thus, these faults mainly controlled the basin configuration during Late Triassic/Early Jurassic period and the uplifted blocks of the faults containing Mesozoic sequences were weathered and eroded before depositing in the grabens over Deccan basalt and Mesozoic succession during Paleocene epoch (Fig. 8). Most of the quartzose sands are derived from stable craton having low relief while presence of high proportion of lithic fragment suggests upliftment at the source area (Dickinson et al. 1983). The craton interior field in the Q-F-L diagram and craton interior to transitional continental field in the Qm-F-Lt plot occupied by these sandstone units suggest a stable craton or passive margin provenance of a rift basin that had supplied sediments to the depositional basin.

Although it is considered that a part of the heavy minerals is altered during diagenesis (e.g. Garzanti and Vezzoli 2003), the abundance of magnetite among the heavy minerals in the studied sandstones suggests that it was derived from a basic igneous rock such as Deccan basalt. Brown tourmaline indicates low rank metamorphic source, while blue tourmaline indicates a pegmatitic source (Pettijohn 1984). The dominance of the brown tourmaline in the MS suggests its derivation from a low-grade metamorphic rock. The occurrence of kyanite in larger proportion and staurolite in smaller proportion suggest that they were contributed from a low- to medium-grade metamorphic source. Rounded grains of rutile, tourmaline and monazite in the studied sandstones were likely derived either from an acid igneous rock or from reworking of the sediments (Pettijohn 1984).

Bipolar paleocurrent patterns are observed in the depositional basins that are influenced by flood- and ebb-tidal currents in a tide-dominated estuarine or deltaic condition (Selley 1980). According to Dalrymple et al. (1992), an estuary is the

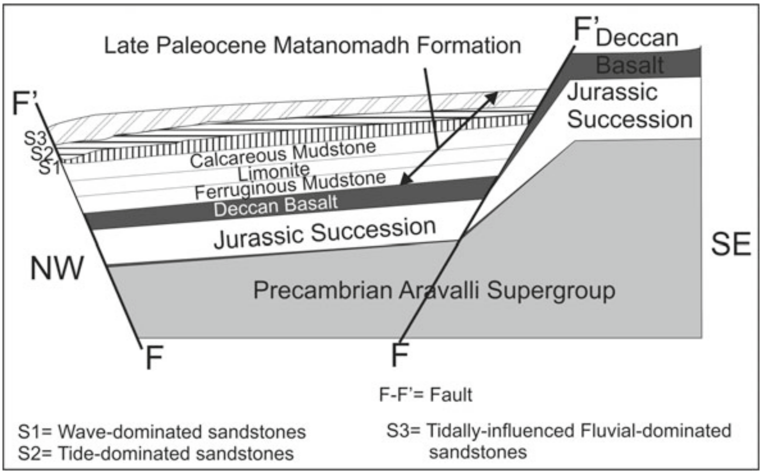

Fig. 8 Cartoon exhibiting vertical distribution of MS lithounits within the late Paleocene half-graven of Kachchh, Gujarat, India and their possible provenance

seaward portion of a drowned valley system which receives sediments from both fluvial and marine sources and which contains facies influenced by marine agents such as tides, waves and fluvial processes. Estuaries may be either tide-dominated or wave-dominated or river-dominated. The bipolar paleocurrent (in parts) suggests that these sandstones were deposited in a wave- and tide-dominated estuary that was later dominated by the unimodal paleocurrent of the fluvial process. The paleocurrent direction for the uppermost tabular cross-bedded sandstone varies slightly than the underlying tangential cross-bedded sandstone, but both are NW-directed. Thus, it is presumed that the NW directed flow was a result of the river current and SE dominated flow was a result of advancing tides. The overall dominance of the WNW paleocurrent direction in the Matanomadh sandstone succession suggests that the main provenance was in the SE direction of the depositional basin. Thus, the Precambrian metamorphic rocks of the basement along with Deccan basalt and Mesozoic sedimentary rocks of the Kachchh basin might have acted as the source during sedimentation of the MS.

Conclusions

Petrographic study of the Matanomadh sandstones shows abundance of sub-angular to rounded monocrystalline non-undulatory quartz in association with minor proportion of feldspar and lithic fragments that classifies them as quartzose arenite variety. The Q-F-L and Qm-F-Lt plots suggest that the sandstones represent craton interior provenance. Abundance of opaque variety of heavy mineral (e.g. magnetite) over the non-opaque tourmaline, kyanite, rutile, monazite and staurolite is observed in these sandstones. The paleocurrents have been bipolar in the lower tide-dominated part of the MS to unidirectional in the upper river-dominated part. The main directions of flow have been NW-SE and WNW, respectively. Petrography and heavy minerals studies along with paleocurrents study suggest that the provenance was dominated by low- to medium-grade metamorphic rocks of the basement i.e. Aravalli metamorphic rocks, volcanic rocks of basaltic composition such as Deccan Trap and older Mesozoic successions exposed in the southeast of the depositional basin.

Acknowledgements The authors are thankful to the Head, Department of Geology, Banaras Hindu University for providing working facilities. Dr. S. K. Ghosh is thanked for going through an earlier version of the manuscript and suggesting modifications.

References

Basu A (1976) Petrology of fluvial sand derived from plutonic source rocks: implications to palaeoclimatic interpretation. J Sediment Petrol 46:694–709

Basu A (2003) A prospective on quantitative provenance analysis. In: Valloni R, Basu A (eds) Quantitative provenance studies in Italy, vol 61. Mem. Deserit. dellacarta Geol. dell Itallia, pp 11–22

Basu A, Molinaroli E (1989) Provenance characteristics of detrital opaque Fe-Ti oxide minerals. J Sediment Petrol 59:922–934

Biswas SK (1965) A new classification of Tertiary rocks of Kachchh, Western India. Bull Geol Min Metall Soc India 35:1–6

Biswas SK (1982) Rift basins in western margin of India with special reference to hydrocarbon prospects. AAPG Bull 66:1497–1513

Biswas SK (1987) Regional tectonic framework, structure and evolution of the western marginal basins of India. Tectonophysics 135:307–327

Biswas SK (1992) Tertiary stratigraphy of Kuth. J Palaeontol Soc India 37:1–29

Biswas SK (2005) A review of structure and tectonics of Kachchh basin, western India, with special reference to earthquakes. Curr Sci 88:1592–1600

Biswas SK, Raju DSN (1973) The rock-stratigraphic classification on the Tertiary sediments of Kachchh. Bull ONGC 10:37–46

Blatt H, Middleton GV, Murray RC (1980) Origin of sedimentary rocks. Prentice Hall, 782 pp

Dalrymple RW, Zaitlin BA, Boyd R (1992) Estuarine facies models: conceptual basis and stratigraphic implications. J Sediment Petrol 62:1130–1146

Dickinson WR, Suczek CA (1979) Plate tectonics and sandstone composition. AAPG Bull 63:2164–2182

Dickinson WR, Beard LS, Brakenridge GR, Erjavek JL, Ferguson RC, Inman KF, Knepp RA, Lindberg FA, Ryberg PT (1983) Provenance of North American Phanerozoic sandstones in relation to tectonic setting. Geol Soc Am Bull 94:222–235

Garzanti E, Vezzoli G (2003) A classification of metamorphic grains in sandstones based on their composition and grade. J Sediment Res 73:830–837

Jalal P, Ghosh SK (2012) Provenance of the Late Neogene Siwalik sandstone, Kumaun Himalayan Foreland Basin: constraints from the metamorphic rank and index of detrital rock fragments. J Earth Syst Sci 121:781–792

Merh SS (1995) Geology of Gujarat. Geol. Soc. India., 220 pp

Morton AC (1985) Heavy minerals in provenance studies. In: Zuffa GG (ed) Provenance of arenites. NATO Advance Science Institute Series, No. 418. D. Reidel, Dordrecht, pp 249–277

Nechaev VP, Isphording WC (1993) Heavy mineral assemblages of continental margins as indicators of plate tectonic environment. J Sediment Petrol 63:1110–1117
Norton IO, Sclater JG (1979) A model for the evolution of the Indian Ocean and the breakup of Gondwanaland. J Geophys Res 84:6803–6830
Okada H (1971) Classification of sandstones: analysis and proposal. J Geol 79:509–525
Patra A, Singh BP, Srivastava VK (2014) Provenance of the late Paleocene sandstones of the Jaisalmer Basin, Western India. J. Geol Soc India 83:657–664
Pettijohn FJ (1984) Sedimentary rocks, 3rd edn. CBS Publishers, 628 pp
Pettijohn FJ, Potter PE, Siever R (1987) Sand and sandstone, 2nd edn. Springer, New York, 553 pp
Saxena RK (1975) Lithostratigraphy of the Matanomadh Formation, Kachchh, India. Palaeobotanist 24:261–262
Selley RC (1980) Ancient sedimentary environments, 2nd edn. Cornell University Press, 287 pp
Singh BP (1996) Murree sedimentation in the northwestern Himalaya. Geol Surv India Spec Publ 21:157–164
Singh BP (2013) Evolution of the Paleogene succession of the western Himalayan foreland basin. Geosci Front 4:199–212
Singh BP, Andotra DS, Kumar R (2000) Provenance of the lower Tertiary mudrocks in the Jammu Sub-Himalayan zone, Jammu and Kashmir State (India), NW Himalaya and its tectonic implications. Geosci J 4:1–9
Singh BP, Pawar JS, Karlupia SK (2004) Dense mineral data from the north-western Himalayan foreland sedimentary rocks and recent river sediments: evaluation of the hinterland. J Asian Earth Sci 23:25–35
Srivastava SK, Pandey N (2011) Search for provenance of Oligocene Barail sandstone in and around Jotsoma, Kohima, Nagaland. J Geol Soc India 77:433–442
Srivastava VK, Singh BP (2017) Shoreface to estuarine sedimentation in the late Paleocene Matanomadh Formation, Kachchh, western India. J Asian Earth Sci 136:1–15
Weltje GJ, Eynatten HV (2004) Quantitative provenance analysis of sediments; review and outlook. Sed Geol 171:1–11
Wynne AB (1872) Geology of Kachchh. Mem Geol Surv India 9:1–289